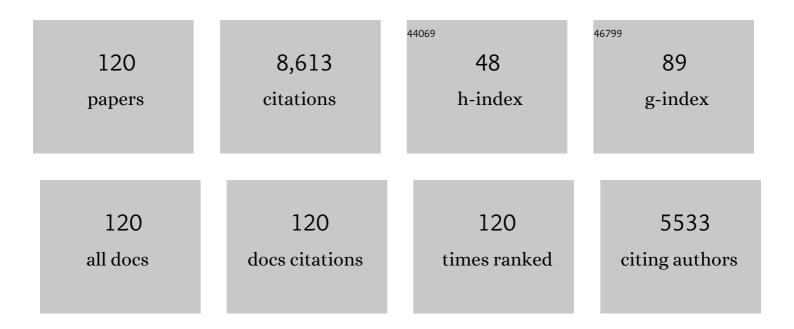


## List of Publications by Year in descending order

Source: https://exaly.com/author-pdf/1074481/publications.pdf Version: 2024-02-01



XINC XII

#	Article	IF	CITATIONS
1	Carbon-based single atom catalyst: Synthesis, characterization, DFT calculations. Chinese Chemical Letters, 2022, 33, 663-673.	9.0	126
2	A 3D MIL-101@rGO composite as catalyst for efficient conversion of straw cellulose into valuable organic acid. Chinese Chemical Letters, 2022, 33, 2573-2578.	9.0	19
3	Insights into selective adsorption mechanism of copper and zinc ions onto biogas residue-based adsorbent: Theoretical calculation and electronegativity difference. Science of the Total Environment, 2022, 805, 150413.	8.0	30
4	Enhanced removal of phosphate using pomegranate peel-modified nickel‑lanthanum hydroxide. Science of the Total Environment, 2022, 809, 151181.	8.0	15
5	A new UV source activates ozone for water treatment: Wavelength-dependent ultraviolet light-emitting diode (UV-LED). Separation and Purification Technology, 2022, 280, 119934.	7.9	11
6	Rational design to manganese and oxygen co-doped polymeric carbon nitride for efficient nonradical activation of peroxymonosulfate and the mechanism insight. Chemical Engineering Journal, 2022, 430, 132751.	12.7	70
7	The enhanced catalytic degradation of sulfamethoxazole over Fe@nitrogen-doped carbon-supported nanocomposite: Insight into the mechanism. Chemical Engineering Journal, 2022, 439, 135784.	12.7	53
8	Boosting fenton-like reaction by reconstructed single Fe atom catalyst for oxidizing organics: Synergistic effect of conjugated π-π sp2 structured carbon and isolated Fe-N4 sites. Chemical Engineering Journal, 2022, 446, 137120.	12.7	45
9	Unveiling the Origins of Selective Oxidation in Single-Atom Catalysis via Co–N <sub>4</sub> –C Intensified Radical and Nonradical Pathways. Environmental Science & Technology, 2022, 56, 11635-11645.	10.0	159
10	Peroxymonosulfate activation on a chainmail catalyst via an electron shuttle mechanism for efficient organic pollutant removal. Applied Catalysis B: Environmental, 2022, 316, 121695.	20.2	33
11	Magnetic field-enhanced radical intensity for accelerating norfloxacin degradation under FeCu/rGO photo-Fenton catalysis. Chemical Engineering Journal, 2021, 420, 127634.	12.7	22
12	Co3O4 anchored in N, S heteroatom co-doped porous carbons for degradation of organic contaminant: role of pyridinic N-Co binding and high tolerance of chloride. Applied Catalysis B: Environmental, 2021, 282, 119484.	20.2	305
13	Degradation of organic pollutants by ultraviolet/ozone in high salinity condition: Non-radical pathway dominated by singlet oxygen. Chemosphere, 2021, 268, 128796.	8.2	32
14	lbuprofen degradation using a Co-doped carbon matrix derived from peat as a peroxymonosulphate activator. Environmental Research, 2021, 193, 110564.	7.5	39
15	Enhanced photodegradation of sulfadimidine via PAA/g-C3N4-Fe0 polymeric catalysts under visible light. Chemical Engineering Journal, 2021, 413, 127456.	12.7	20
16	A tunable amphiphilic Enteromorpha-modified graphene aerogel for oil/water separation. Science of the Total Environment, 2021, 763, 142958.	8.0	47
17	Flocculation behaviors of a novel papermaking sludge-based flocculant in practical printing and dyeing wastewater treatment. Frontiers of Environmental Science and Engineering, 2021, 15, 1.	6.0	17
18	Single-atom catalysis in advanced oxidation processes for environmental remediation. Chemical Society Reviews, 2021, 50, 5281-5322.	38.1	502

#	Article	IF	CITATIONS
19	Improving peroxymonosulfate activation by copper ion-saturated adsorbent-based single atom catalysts for the degradation of organic contaminants: electron-transfer mechanism and the key role of Cu single atoms. Journal of Materials Chemistry A, 2021, 9, 11604-11613.	10.3	85
20	Preferential capture of phosphate by an Enteromorpha prolifera–based biopolymer encapsulating hydrous zirconium oxide nanoparticles. Environmental Science and Pollution Research, 2021, 28, 34584-34597.	5.3	1
21	Highly efficient removal of phosphate from aqueous media by pomegranate peel co-doping with ferric chloride and lanthanum hydroxide nanoparticles. Journal of Cleaner Production, 2021, 292, 125311.	9.3	25
22	Novel lignin-based single atom catalysts as peroxymonosulfate activator for pollutants degradation: Role of single cobalt and electron transfer pathway. Applied Catalysis B: Environmental, 2021, 286, 119910.	20.2	209
23	Engineered carbon supported single iron atom sites and iron clusters from Fe-rich Enteromorpha for Fenton-like reactions via nonradical pathways. Applied Catalysis B: Environmental, 2021, 287, 119963.	20.2	271
24	Application of sectionalized single-step reaction approach (SSRA) and distributed activation energy model (DAEM) on the pyrolysis kinetics model of upstream oily sludge: Construction procedure and data reproducibility comparison. Science of the Total Environment, 2021, 774, 145751.	8.0	11
25	Effective removal of hexavalent chromium from aqueous solution by ZnCl2 modified biochar: Effects and response sequence of the functional groups. Journal of Molecular Liquids, 2021, 334, 116149.	4.9	41
26	Fabrication of graphitic carbon nitride functionalized P–CoFe2O4 for the removal of tetracycline under visible light: Optimization, degradation pathways and mechanism evaluation. Chemosphere, 2021, 274, 129783.	8.2	38
27	Recycling exhausted magnetic biochar with adsorbed Cu2+ as a cost-effective permonosulfate activator for norfloxacin degradation: Cu contribution and mechanism. Journal of Hazardous Materials, 2021, 413, 125413.	12.4	87
28	The application of UV/O3 process on ciprofloxacin wastewater containing high salinity: Performance and its degradation mechanism. Chemosphere, 2021, 276, 130220.	8.2	42
29	Effect of phosphate on peroxymonosulfate activation: Accelerating generation of sulfate radical and underlying mechanism. Applied Catalysis B: Environmental, 2021, 298, 120532.	20.2	172
30	Activation of peroxymonosulfate via mediated electron transfer mechanism on single-atom Fe catalyst for effective organic pollutants removal. Applied Catalysis B: Environmental, 2021, 299, 120714.	20.2	173
31	One-step synthesis of "nuclear-shell―structure iron-carbon nanocomposite as a persulfate activator for bisphenol A degradation. Chemical Engineering Journal, 2020, 382, 122780.	12.7	77
32	Enhanced As(Đ <sup>°°</sup> ) removal from aqueous solutions by recyclable Cu@MNM composite membranes via synergistic oxidation and absorption. Water Research, 2020, 168, 115147.	11.3	53
33	Sulfate saturated biosorbent-derived Co-S@NC nanoarchitecture as an efficient catalyst for peroxymonosulfate activation. Applied Catalysis B: Environmental, 2020, 262, 118302.	20.2	289
34	Modified biogas residues as an eco-friendly and easily-recoverable biosorbent for nitrate and phosphate removals from surface water. Journal of Hazardous Materials, 2020, 382, 121073.	12.4	56
35	Co-monomer polymer anion exchange resin for removing Cr(VI) contaminants: Adsorption kinetics, mechanism and performance. Science of the Total Environment, 2020, 709, 136002.	8.0	56
36	Highly-efficient degradation of triclosan attributed to peroxymonosulfate activation by heterogeneous catalyst g-C3N4/MnFe2O4. Chemical Engineering Journal, 2020, 391, 123554.	12.7	70

#	Article	IF	CITATIONS
37	Synthesis, characterization and flocculation performance of a novel sodium alginate-based flocculant. Carbohydrate Polymers, 2020, 248, 116790.	10.2	35
38	Structure-activity relationships of the papermill sludge-based flocculants in different dye wastewater treatment. Journal of Cleaner Production, 2020, 266, 121944.	9.3	17
39	Three-dimensional porous graphene-like biochar derived from Enteromorpha as a persulfate activator for sulfamethoxazole degradation: Role of graphitic N and radicals transformation. Journal of Hazardous Materials, 2020, 399, 123039.	12.4	152
40	Effects of charge density and molecular weight of papermaking sludge-based flocculant on its decolorization efficiencies. Science of the Total Environment, 2020, 723, 138136.	8.0	8
41	Highly efficient and mild electrochemical degradation of bentazon by nano-diamond doped PbO2 anode with reduced Ti nanotube as the interlayer. Journal of Colloid and Interface Science, 2020, 575, 254-264.	9.4	48
42	Mechanism of sonication time on structure and adsorption properties of 3D peanut shell/graphene oxide aerogel. Science of the Total Environment, 2020, 739, 139983.	8.0	24
43	Nitrogen-doped carbon nanotubes encapsulating Fe/Zn nanoparticles as a persulfate activator for sulfamethoxazole degradation: role of encapsulated bimetallic nanoparticles and nonradical reaction. Environmental Science: Nano, 2020, 7, 1444-1453.	4.3	113
44	Waste-to-resources: Green preparation of magnetic biogas residues-based biochar for effective heavy metal removals. Science of the Total Environment, 2020, 737, 140283.	8.0	52
45	Enhanced degradation of clothianidin in peroxymonosulfate/catalyst system via core-shell FeMn @ N-C and phosphate surrounding. Applied Catalysis B: Environmental, 2020, 267, 118717.	20.2	267
46	Single and Binary Competitive Adsorption of Cobalt and Nickel onto Novel Magnetic Composites Derived from Green Macroalgae. Environmental Engineering Science, 2020, 37, 188-200.	1.6	12
47	Adsorptive removal of phosphate by the bimetallic hydroxide nanocomposites embedded in pomegranate peel. Journal of Environmental Sciences, 2020, 91, 189-198.	6.1	23
48	Co/Fe and Co/Al layered double oxides ozone catalyst for the deep degradation of aniline: Preparation, characterization and kinetic model. Science of the Total Environment, 2020, 715, 136982.	8.0	73
49	Effect of washing conditions on adsorptive properties of mesoporous silica carbon composites by in-situ carbothermal treatment. Science of the Total Environment, 2020, 716, 136770.	8.0	8
50	Alleviating membrane fouling of modified polysulfone membrane via coagulation pretreatment/ultrafiltration hybrid process. Chemosphere, 2019, 235, 58-69.	8.2	37
51	A facile approach to ultralight and recyclable 3D self-assembled copolymer/graphene aerogels for efficient oil/water separation. Science of the Total Environment, 2019, 694, 133671.	8.0	46
52	One-step synthesis of easily-recoverable carboxylated biogas residues for efficient removal of heavy metal ions from synthetic wastewater. Journal of Cleaner Production, 2019, 240, 118264.	9.3	24
53	Removal of sulfamethoxazole from water via activation of persulfate by Fe3C@NCNTs including mechanism of radical and nonradical process. Chemical Engineering Journal, 2019, 375, 122004.	12.7	244
54	Preparation of Cu2O-Fe3O4@carbon nanocomposites derived from natural polymer hydrogel template for organic pollutants degradation. Journal of the Taiwan Institute of Chemical Engineers, 2019, 102, 456-464.	5.3	12

#	Article	IF	CITATIONS
55	Synthesis of polyaluminium chloride/papermaking sludge-based organic polymer composites for removal of disperse yellow and reactive blue by flocculation. Chemosphere, 2019, 231, 337-348.	8.2	35
56	Multiple bimetallic (Al-La or Fe-La) hydroxides embedded in cellulose/graphene hybrids for uptake of fluoride with phosphate surroundings. Journal of Hazardous Materials, 2019, 379, 120634.	12.4	31
57	Enhanced fluoride uptake by bimetallic hydroxides anchored in cotton cellulose/graphene oxide composites. Journal of Hazardous Materials, 2019, 376, 91-101.	12.4	33
58	In-situ pyrolysis of Enteromorpha as carbocatalyst for catalytic removal of organic contaminants: Considering the intrinsic N/Fe in Enteromorpha and non-radical reaction. Applied Catalysis B: Environmental, 2019, 250, 382-395.	20.2	418
59	Fe/Mn nanoparticles encapsulated in nitrogen-doped carbon nanotubes as a peroxymonosulfate activator for acetamiprid degradation. Environmental Science: Nano, 2019, 6, 1799-1811.	4.3	197
60	Selective removal of phosphate by dual Zr and La hydroxide/cellulose-based bio-composites. Journal of Colloid and Interface Science, 2019, 533, 692-699.	9.4	62
61	Column adsorption and regeneration study of magnetic biopolymer resin for perchlorate removal in presence of nitrate and phosphate. Journal of Cleaner Production, 2019, 213, 762-775.	9.3	49
62	Development of combined coagulation-hydrolysis acidification-dynamic membrane bioreactor system for treatment of oilfield polymer-flooding wastewater. Frontiers of Environmental Science and Engineering, 2019, 13, 1.	6.0	13
63	Insights into the phosphate adsorption behavior onto 3D self-assembled cellulose/graphene hybrid nanomaterials embedded with bimetallic hydroxides. Science of the Total Environment, 2019, 653, 897-907.	8.0	46
64	Evaluation of molecular weight, chain architectures and charge densities of various lignin-based flocculants for dye wastewater treatment. Chemosphere, 2019, 215, 214-226.	8.2	51
65	One-step synthesis of peanut hull/graphene aerogel for highly efficient oil-water separation. Journal of Cleaner Production, 2019, 207, 764-771.	9.3	89
66	A wheat straw cellulose-based hydrogel for Cu (II) removal and preparation copper nanocomposite for reductive degradation of chloramphenicol. Carbohydrate Polymers, 2018, 190, 12-22.	10.2	45
67	Three-dimensional reduced graphene oxide/carbon nanotube nanocomposites anchoring of amorphous and crystalline molybdenum sulfide: Physicochemical characteristics and electrocatalytic hydrogen evolution performances. Electrochimica Acta, 2018, 273, 402-411.	5.2	19
68	Application and mechanism of polysaccharide extracted from Enteromorpha to remove nano-ZnO and humic acid in coagulation process. Frontiers of Environmental Science and Engineering, 2018, 12, 1.	6.0	9
69	Adsorption of phosphate by the cellulose-based biomaterial and its sustained release of laden phosphate in aqueous solution and soil. International Journal of Biological Macromolecules, 2018, 109, 524-534.	7.5	44
70	Bio-reduction of free and laden perchlorate by the pure and mixed perchlorate reducing bacteria: Considering the pH and coexisting nitrate. Chemosphere, 2018, 205, 475-483.	8.2	11
71	rGO/CNTs Supported Pyrolysis Derivatives of [Mo <sub>3</sub> S <sub>13</sub> ] <sup>2–</sup> Clusters as Promising Electrocatalysts for Enhancing Hydrogen Evolution Performances. ACS Sustainable Chemistry and Engineering, 2018, 6, 6920-6931.	6.7	17
72	Study on the treatment of soybean protein wastewater by a pilot-scale IC-A/O coupling reactor. Chemical Engineering Journal, 2018, 343, 189-197.	12.7	22

#	Article	IF	CITATIONS
73	Cellulose based multifunctional hybrid material for sequestering phosphate in stratified water purification columns. Cellulose, 2018, 25, 5877-5892.	4.9	4
74	Removal of fluoride by carbohydrate-based material embedded with hydrous zirconium oxide nanoparticles. Environmental Science and Pollution Research, 2018, 25, 27982-27991.	5.3	14
75	Highly selective and efficient removal of fluoride from aqueous solution by Zr La dual-metal hydroxide anchored bio-sorbents. Journal of Cleaner Production, 2018, 199, 36-46.	9.3	45
76	Uptake of phosphate and Cr(VI) by amine-functionalized Chinese reed: Considering the computations and characteristics analysis. Journal of the Taiwan Institute of Chemical Engineers, 2017, 72, 85-94.	5.3	7
77	Bio-regeneration of spent Fe 3 O 4 laden quaternary-ammonium shaddock peel after perchlorate capture: Considering the oxygen, coexisting anions, bio-fouling and indirect bio-regeneration. Chemical Engineering Journal, 2017, 316, 204-213.	12.7	10
78	Preferable uptake of phosphate by hydrous zirconium oxide nanoparticles embedded in quaternary-ammonium Chinese reed. Journal of Colloid and Interface Science, 2017, 496, 118-129.	9.4	53
79	Biosorption and Bioreduction of Perchlorate Using the Nano-Fe <sub>3</sub> O <sub>4</sub> -Laden Quaternary-Ammonium Chinese Reed: Considering the Coexisting Nitrate and Nano-Fe <sub>3</sub> O <sub>4</sub> . ACS Sustainable Chemistry and Engineering, 2017, 5, 2471-2482.	6.7	20
80	Integration of coagulation and adsorption for removal of N-nitrosodimethylamine (NDMA) precursors from biologically treated municipal wastewater. Environmental Science and Pollution Research, 2017, 24, 12426-12436.	5.3	7
81	Application for oxytetracycline wastewater pretreatment by Fenton iron mud based cathodic-anodic-electrolysis ceramic granular fillers. Chemosphere, 2017, 182, 483-490.	8.2	23
82	Effective adsorption/desorption of perchlorate from water using corn stalk based modified magnetic biopolymer ion exchange resin. Microporous and Mesoporous Materials, 2017, 252, 59-68.	4.4	31
83	The rapid adsorption-microbial reduction of perchlorate from aqueous solution by novel amine-crosslinked magnetic biopolymer resin. Bioresource Technology, 2017, 240, 68-76.	9.6	22
84	Amine-crosslinked Shaddock Peel embedded with hydrous zirconium oxide nano-particles for selective phosphate removal in competitive condition. Journal of the Taiwan Institute of Chemical Engineers, 2017, 80, 650-662.	5.3	22
85	Thiomolybdate [Mo <sub>3</sub> S <sub>13</sub> 2– Nanoclusters Anchored on Reduced Graphene Oxide-Carbon Nanotube Aerogels for Efficient Electrocatalytic Hydrogen Evolution. ACS Sustainable Chemistry and Engineering, 2017, 5, 8908-8917.	6.7	42
86	Capture of perchlorate by a surface-modified bio-sorbent and its bio-regeneration properties: Adsorption, computations and biofouling. Chemosphere, 2017, 185, 152-161.	8.2	7
87	Novel cationic polyamidine: Synthesis, characterization, and sludge dewatering performance. Journal of Environmental Sciences, 2017, 51, 305-314.	6.1	22
88	Removal of phosphate and chromium( <scp>vi</scp> ) from liquids by an amine-crosslinked nano-Fe <sub>3</sub> O <sub>4</sub> biosorbent derived from corn straw. RSC Advances, 2016, 6, 47237-47248.	3.6	62
89	Adsorption–desorption behavior of magnetic amine/Fe3O4 functionalized biopolymer resin towards anionic dyes from wastewater. Bioresource Technology, 2016, 210, 123-130.	9.6	175
90	FTIR, Raman, and XPS analysis during phosphate, nitrate and Cr(VI) removal by amine cross-linking biosorbent. Journal of Colloid and Interface Science, 2016, 468, 313-323.	9.4	230

#	Article	IF	CITATIONS
91	Removal of anionic pollutants from liquids by biomass materials: A review. Journal of Molecular Liquids, 2016, 215, 565-595.	4.9	125
92	Adsorption of nitrate from aqueous solution by magnetic amine-crosslinked biopolymer based corn stalk and its chemical regeneration property. Journal of Hazardous Materials, 2016, 304, 280-290.	12.4	138
93	Adsorption of phosphate on surface of magnetic reed: characteristics, kinetic, isotherm, desorption, competitive and mechanistic studies. RSC Advances, 2016, 6, 5089-5099.	3.6	15
94	Treatment of dissolved perchlorate by adsorption–microbial reduction. Chemical Engineering Journal, 2015, 279, 522-529.	12.7	23
95	High-capacity adsorption of dissolved hexavalent chromium using amine-functionalized magnetic corn stalk composites. Bioresource Technology, 2015, 190, 550-557.	9.6	103
96	Performance of novel biopolymer-based activated carbon and resin on phosphate elimination from stream. Colloids and Surfaces A: Physicochemical and Engineering Aspects, 2015, 476, 68-75.	4.7	31
97	Integration of adsorption and direct bio-reduction of perchlorate on surface of cotton stalk based resin. Journal of Colloid and Interface Science, 2015, 459, 127-135.	9.4	22
98	Study of microbial perchlorate reduction: Considering of multiple pH, electron acceptors and donors. Journal of Hazardous Materials, 2015, 285, 228-235.	12.4	44
99	Physicochemical characteristics of epichlorohydrin, pyridine and trimethylamine functionalized cotton stalk and its adsorption/desorption properties for perchlorate. Journal of Colloid and Interface Science, 2015, 440, 219-228.	9.4	23
100	Column adsorption of perchlorate by amine-crosslinked biopolymer based resin and its biological, chemical regeneration properties. Carbohydrate Polymers, 2015, 115, 432-438.	10.2	45
101	Removal of Cu(II) and Cr(VI) from wastewater by an amphoteric sorbent based on cellulose-rich biomass. Carbohydrate Polymers, 2014, 111, 788-796.	10.2	94
102	Uptake of perchlorate from aqueous solutions by amine-crosslinked cotton stalk. Carbohydrate Polymers, 2013, 98, 132-138.	10.2	32
103	Characteristics of Amine Surfactant Modified Peanut Shell and Its Sorption Property for Cr(VI). Chinese Journal of Chemical Engineering, 2013, 21, 1260-1268.	3.5	28
104	Nitrate adsorption by multiple biomaterial based resins: Application of pilot-scale and lab-scale products. Chemical Engineering Journal, 2013, 234, 397-405.	12.7	50
105	Nitrate adsorption by stratified wheat straw resin in lab-scale columns. Chemical Engineering Journal, 2013, 226, 1-6.	12.7	82
106	Perchlorate uptake by wheat straw based adsorbent from aqueous solution and its subsequent biological regeneration. Chemical Engineering Journal, 2012, 211-212, 37-45.	12.7	34
107	Adsorption of hexavalent chromium from aqueous solution by modified corn stalk: A fixed-bed column study. Bioresource Technology, 2012, 113, 114-120.	9.6	403
108	Nitrate removal from aqueous solution by Arundo donax L. reed based anion exchange resin. Journal of Hazardous Materials, 2012, 203-204, 86-92.	12.4	70

#	Article	IF	CITATIONS
109	Characteristics of diethylenetriamine-crosslinked cotton stalk/wheat stalk and their biosorption capacities for phosphate. Journal of Hazardous Materials, 2011, 192, 1690-1696.	12.4	78
110	Characteristics of amine-crosslinked wheat straw and its adsorption mechanisms for phosphate and chromium (VI) removal from aqueous solution. Carbohydrate Polymers, 2011, 84, 1054-1060.	10.2	88
111	Sorption of phosphate onto giant reed based adsorbent: FTIR, Raman spectrum analysis and dynamic sorption/desorption properties in filter bed. Bioresource Technology, 2011, 102, 5278-5282.	9.6	64
112	Preparation and characteristics of anion exchanger from corn stalks. Desalination, 2011, 274, 113-119.	8.2	26
113	Sorption of nitrate onto amine-crosslinked wheat straw: Characteristics, column sorption and desorption properties. Journal of Hazardous Materials, 2011, 186, 206-211.	12.4	61
114	Characteristics of cellulosic amine-crosslinked copolymer and its sorption properties for Cr(VI) from aqueous solutions. Journal of Hazardous Materials, 2011, 189, 420-426.	12.4	57
115	Preparation of agricultural by-product based anion exchanger and its utilization for nitrate and phosphate removal. Bioresource Technology, 2010, 101, 8558-8564.	9.6	124
116	Adsorption studies of the removal of anions from aqueous solutions onto an adsorbent prepared from wheat straw. Science China Chemistry, 2010, 53, 1414-1419.	8.2	6
117	Preparation and utilization of wheat straw bearing amine groups for the sorption of acid and reactive dyes from aqueous solutions. Journal of Hazardous Materials, 2010, 182, 1-9.	12.4	92
118	Optimized conditions in preparation of giant reed quaternary amino anion exchanger for phosphate removal. Chemical Engineering Journal, 2010, 157, 161-167.	12.7	49
119	Effect of modifying agents on the preparation and properties of the new adsorbents from wheat straw. Bioresource Technology, 2010, 101, 1477-1481.	9.6	29
120	Adsorption of phosphate from aqueous solutions onto modified wheat residue: Characteristics, kinetic and column studies. Colloids and Surfaces B: Biointerfaces, 2009, 70, 46-52.	5.0	94